J. Am. Chem. Soc. **1993**, *115*, 5783–5789

The $C_4H_8^{\bullet+}$ Potential Energy Surface. 2. The $(C_2H_4)_2^{\bullet+}$ Complex Cation and Its Reaction to the Radical Cations of Cyclobutane and 1-Butene

Pavel Jungwirth[†] and Thomas Bally[*]

Contribution from the Institute of Physical Chemistry, University of Fribourg, Pérolles, 1700 Fribourg, Switzerland

Received September 22, 1992

Abstract: The reaction of ethylene (Et) and its radical cation ($Et^{\bullet+}$), which has received much attention from the experimental side, was studied at the QCISD(T)/6-31G*//UMP2/6-31G* level of theory. According to these calculations the primary product of this reaction is a π complex cation $[Et\cdots Et]^{\bullet+}$, where the two Et molecules are linked by a single bond of $\approx$1.9 Å and which is bound by 18.2 kcal/mol relative to Et + $Et^{\bullet+}$, in good agreement with experiment. Starting from this complex, two transition states were located, one leading to the radical cation of cyclobutane (E_a = 9.0 kcal/mol) and the other involving a 1,3 H-shift leading to the radical cation of 1-butene (E_a = 5.9 kcal/mol). No equilibrium structure corresponding to the frequently postulated tightly bound tetramethylene radical cation intermediate could be found, and therefore no such species seems to be involved in the well-documented rearrangements of $[Et\cdots Et]^{\bullet+}$ and/or ionized cyclobutane to butene radical cations. An intriguing discrepancy between the minimum-energy structures of the $[Et\cdots Et]^{\bullet+}$ complex on the UHF and the UMP2 potential energy surfaces is discussed in terms of a bias introduced by the poor convergence of the Møller–Plesset perturbation series for species whose UHF wave function is strongly contaminated by higher spin states. A revised picture of the potential energy surfaces on which the various $C_4H_4^{\bullet+}$ rearrangements which were observed both in the gas phase and in condensed phase is proposed.

1. Introduction

(a) Gas-Phase Studies. The ion–molecule reaction between ethylene (Et) and its radical cation ($Et^{\bullet+}$) is among the most extensively studied processes of its kind.[1a,b] Most gas-phase experiments centered on the mode of formation of the allylic ions, $C_3H_5^+$ and $C_4H_7^+$, which are also prominent charged fragments in the mass spectra of various C_4H_8 isomers. There is now general agreement that fragmentation is preceded by an efficient rearrangement of the incipient $(Et\cdots Et)^{\bullet+}$ collision complex to a tightly bound $C_4H_8^{\bullet+}$ species which lives long enough to allow for complete randomization of the internal energy prior to dissociation.[1c,d] High-pressure experiments in which these molecules were relieved of their excess energy and neutralized by charge exchange with appropriate donors revealed mainly 2-butene (2B) and isobutene (iB) as isolable products which served as a clue to the identity of the ionic $C_4H_8^{\bullet+}$ precursors.[2]

The same products were also found after reneutralization of $C_4H_8^{\bullet+}$ obtained by static radiolysis[3] or photoionization[4] of cyclobutane (CB) under conditions where little or no fragmentation occurs. Ensuing studies showed that the threshold for charge exchange of $C_4H_8^{\bullet+}$ formed in this way ($\geq$9.3 eV) was only compatible with butene structures, which proved that the rearrangement had taken place prior to reneutralization.[5] Furthermore, reaction of $C_4H_8^{\bullet+}$ with C_6D_{12} was found to produce 80% *n*-butane-*2,3*-d_2 and 20% 2-methylpropane-*1,2*-d_2, which served as an indication of the $2B^{\bullet+}/iB^{\bullet+}$ ratio.[6]

Later investigations focused on the details of the mechanism for the rearrangements of ionized CB[7] or $(Et\cdots Et)$[1a,8] by endowing the precursor ions with variable and well-defined amounts of excess energy. Thus, appearance energies[1a,8a] and/or breakdown graphs[7,8b] for the formation of the two allylic fragments were obtained, and these findings were interpreted by statistical thermodynamic models under various assumptions regarding the nature of possible intermediates.[7,8a,9] Thereby it was invariably concluded that $CB^{\bullet+}$ isomerizes (or fragments) via a tetramethylene radical cation[7] ($tM^{\bullet+}$), which was also postulated as an intermediate between the loose $(Et\cdots Et)^{\bullet+}$ complex and the more stable butene cations.[1c,8,9] Very recently, Shinohara et al. contributed a study where $(Ar)_m\cdot(Et)_n^{\bullet+}$ clusters were stabilized by "intracluster energy dissipation" (evaporation of Ar and Et), and these authors claim to have observed for the first time the thermalized $(Et\cdots Et)^{\bullet+}$ complex.[10]

Figure 1 summarizes schematically the state of knowledge about the formation and the main fragmentation paths of $C_4H_8^{\bullet+}$ obtained from Et + $Et^{\bullet+}$ and/or $CB^{\bullet+}$ using experimental thermochemical data where those are available.[11] Since the butene cations were invariably formed with substantial amounts of excess energy, the above mentioned experiments did not yield any indications regarding the rearrangement of the differen isomers and it was concluded that they interconvert rapidly prior to fragmentation.

---

[*] To whom correspondence should be addressed.

[†] On leave from J. Heyrovský Institute of Physical Chemistry and Electrochemistry, Academy of Sciences of the Czech Republic, Dolejskova 3, 182 23 Prague 8, Czech Republic.

(1) (a) Ono, Y.; Linn, S. H.; Tzeng, W.-B.; Ng, C. Y. *J. Chem. Phys.* **1984**, *80*, 1482. (b) This paper quotes 30 references on the subject even though it excludes some of the earliest ones. (c) Lee, A.; Leroy, R. L.; Herman, Z.; Wolfgang, R.; Tully, J. C. *Chem. Phys. Lett.* **1972**, *12*, 569. (d) Le Breton, P. R.; Williamson, A. D.; Beauchamp, J. L.; Huntress, W. T. *J. Chem. Phys.* **1975**, *62*, 1623.

(2) (a) Meisels, G. G. *J. Chem. Phys.* **1965**, *42*, 3239. (b) Gorden, R.; Ausloos, P. *J. Chem. Phys.* **1967**, *47*, 1799. (c) Gill, P. S.; Inel, Y.; Meisels, G. G. *J. Chem. Phys.* **1971**, *54*, 2811.

(3) Doepker, R. D.; Ausloos, P. *J. Chem. Phys.* **1966**, *44*, 1641.

(4) Doepker, R. D.; Ausloos, P. *J. Chem. Phys.* **1965**, *43*, 3814.

(5) Hughes, B. M.; Tiernan, T. O. *J. Chem. Phys.* **1969**, *51*, 4337.

(6) Sieck, L. W.; Searles, S. K.; Ausloos, P. *J. Am. Chem. Soc.* **1969**, *91*, 7627.

(7) (a) Lifshitz, C.; Tiernan, T. O. *J. Chem. Phys.* **1971**, *55*, 3555. (b) Hsieh, T.; Gilman, J. P.; Weiss, M. J.; Meisels, G. G. *J. Phys. Chem.* **1981**, *85*, 2722.

(8) (a) Ceyer, S. T.; Tiedemann, P. W.; Ng, C. Y.; Mahan, B. H.; Lee, Y. T. *J. Chem. Phys.* **1979**, *70*, 2138. (b) Van der Meij, C. E.; Van Eck, J.; Niehaus, A. *Chem. Phys.* **1989**, *130*, 325.

(9) Chesnavich, W. J.; Bass, L.; Su, T.; Bowers, M. T. *J. Chem. Phys.* **1981**, *70*, 2138.

(10) Shinohara, H.; Sato, H.; Washida, N. *J. Phys. Chem.* **1990**, *94*, 6718.

(11) In ref 1a a critical compilation of the thermochemical data relevant to the formation and fragmentation of $C_4H_4^{\bullet+}$ is given from which the values in Figure 1 were taken.

0002-7863/93/1515-5783$04.00/0 © 1993 American Chemical Society

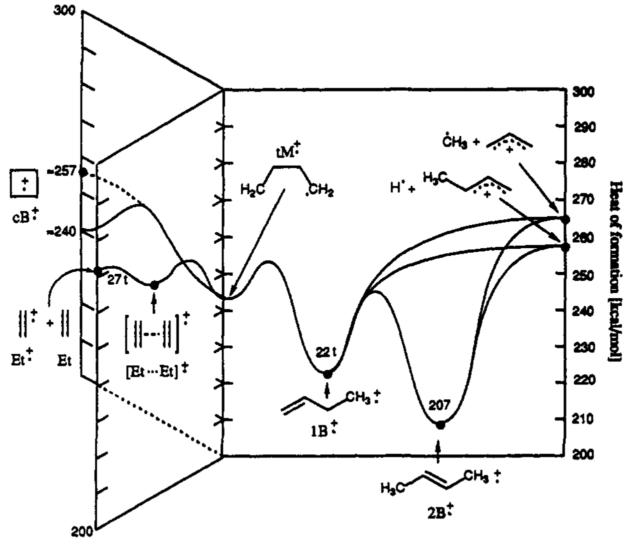

Figure 1. Qualitative picture of the $C_4H_8^{\bullet+}$ potential energy surface as it emerges from gas-phase studies of ionized cyclobutane and ethylene dimers. Filled dots correspond to experimental thermochemical data.[1a] The entry channel for ionized cyclobutane (dashed line) was placed at the energy where it is situated after 1165-Å (10.68 eV) photolysis.[2b,c]

(b) Condensed-Phase Studies. On a different front, the same species (or derivatives thereof) were observed in various condensed-phase experiments. Thus, it was found that tetramethylethylene (Me_4Et) forms stable dimer[12] or higher cluster cations[13] of the classical π-sandwich type discernible by their ESR spectra as well as by their characteristic NIR "charge resonance" band,[14] which in the case of $(Me_4Et)_2^{\bullet+}$ peaks at 860 nm.[12] Conversely, Fujisawa et al. showed that, upon ionization of parent ethylene (Et) in Freon matrices, the first product identifiable by ESR is the radical cation of 1-butene ($1B^{\bullet+}$),[15] which can be converted photolytically to $2B^{\bullet+}$ or reacted with further Et upon annealing the matrix. On the other hand, it was demonstrated by another Japanese group that cyclobutane radical cation ($CB^{\bullet+}$), which is stable in Freon matrices,[16] undergoes a photorearrangement to $1B^{\bullet+}$ (and later $2B^{\bullet+}$).[17] The authors of this work concluded that $tM^{\bullet+}$ (which they presumed to be the primary photoproduct) was unstable under their experimental conditions.

Finally, Ledwith found that certain vinyl-substituted aromatic amines engage readily in [1 + 2] cycloadditions to yield the corresponding cyclobutanes under the catalytic influence of suitable one-electron oxidants or photoexcited sensitizers known to undergo single-electron transfer upon quenching.[18] Later studies revealed an analogous behavior of other electron-rich olefins.[19] Interestingly, some of the cyclobutanes formed in this way were also found to undergo ring *opening* upon oxidation,[20] and since 1,4-dimethoxybutanes were recovered from reactions in methanol, it was concluded that tetramethylene radical cations were crucial intermediates both in the cleavage and the (stepwise) formation of electron-rich cyclobutane derivatives. In cases where the oxidation potential of the cyclobutane exceeds that of the precursor olefin,[21] the cyclodimerization can even be run as a chain process.[18]

The [2 + 1] cycloaddition process also received much attention by Bauld et al.,[22] who subsequently engaged in pioneering theoretical calculations to shed light on the mechanism of this formally symmetry-forbidden process. Bauld showed in particular that ion–molecule reactions involving certain acyclic dienes which lead to formal Diels–Alder type adducts may actually proceed in two stages, i.e. a cyclobutanation followed by a vinylcyclobutane rearrangement.

(c) Previous Theoretical Work. In view of the intense activity in the experimental field, surprisingly few attempts were made to apply quantum chemical models to those sections of the $C_4H_8^{\bullet+}$ potential energy surface (P.E.S.) relevant to the above described studies. In 1975, Almlöf et al.[23] showed by ab initio calculations with a split valence basis set that the Et + $Et^{\bullet+}$ reaction led to a π-complex of (assumed) D_{2h} symmetry where charge and spin were distributed evenly between the two partners, in agreement with the ESR data on the tetramethyl derivative.[12] They calculated a dissociation energy of 0.62 eV for the $(Et\cdots Et)^{\bullet+}$ π-complex under the assumption that the C–C bond length is 1.365 Å.

Bauld et al. carried the theoretical treatment of the Et + $Et^{\bullet+}$ reaction one step further by investigating the mechanism of the cyclobutane formation. They noted that the [2 + 1] cycloaddition is symmetry forbidden as a synchronous process but that the retention of stereochemistry found for the radical-cation-catalyzed cyclobutanation of electron-rich olefins[24a] requires some concert in the formation of the two bonds. Thus, they investigated the reaction path by MNDO[24b] and later also by ab initio calculations[24c] which were interpreted to support this conjecture: MNDO predicted initial formation of a stable $tM^{\bullet+}$ intermediate,[24b] but this result was dismissed as spurious due to the known tendency of MNDO to favor stepwise pathways for neutral pericyclic reactions which are known to occur concertedly. On the other hand, UHF/3-21G geometry optimizations[24c] led with no activation to a loose π-complex (r_{14} = 2.227 Å, r_{23} = 3.062 Å) 19.8 kcal/mol below the separated fragments (14.2 kcal/mol by single-point UHF/6-31G* calculations) which cyclizes to $CB^{\bullet+}$ in a concerted way with an activation energy of 7.1 (7.4) kcal/mol.[24d] Since, the transition state for cyclobutanation was lower than the energy of the separated fragments, they concluded that the [2 + 1] cycloaddition occurs in fact with no activation.

More recently, Chandra et al. recalculated the binding energy of an idealized $(Et\cdots Et)^{\bullet+}$ π-complex by correcting for the basis set superposition error (BSSE) with the counterpoise procedure and by calculating the dispersion contribution explicitly.[25] This led them to a predicted dissociation energy of 22.5 kcal/mol and an equilibrium distance of 2.5 Å. Finally, Lee et al. devoted an elaborate study to the Et + $Et^{\bullet+}$ cycloaddition, relying on quasiadiabatic surface analyses to obtain a qualitative picture of the state-symmetry changes which take place during this process if certain symmetry elements are preserved.[26] Their quantitative calculations confirmed essentially the results of Bauld et al. except that they found a nearly rectangular structure at the transition state for final cyclization.

---

(12) (a) Ichikawa, T.; Ludwig, P. K. *J. Am. Chem. Soc.* **1969**, *91*, 1023. (b) Ichikawa, T.; Ohta, N.; Kajioka, H. *J. Phys. Chem.* **1979**, *83*, 284. (c) Barnabas, M. V.; Trifunac, A. D. *Chem. Phys. Lett.* **1992**, *193*, 298.

(13) Desrosiers, M. F.; Trifunac, A. D. *J. Phys. Chem.* **1986**, *90*, 1560.

(14) Badger, B.; Brocklehurst, B. *Trans. Faraday Soc.* **1966**, *66*, 2939.

(15) Fujisawa, J.; Sato, S.; Shimokoshi, K. *Chem. Phys. Lett.* **1986**, *124*, 391.

(16) Ushida, K.; Shida, T.; Iwasaki, M.; Toriyama, K.; Nunome, J. *J. Am. Chem. Soc.* **1983**, *105*, 5496.

(17) Toriyama, K.; Nunome, K.; Iwasaki, M.; Shida, T.; Ushida, K. *Chem. Phys. Lett.* **1985**, *122*, 118.

(18) Ledwith, A. *Acc. Chem. Res.* **1972**, *5*, 133.

(19) See: Mattes, S. L.; Farid, S. *Acc. Chem. Res.* **1982**, *15*, 80.

(20) Beresford, P.; Lambert, M. C.; Ledwith, A. *J. Chem. Soc. C* **1970**, 2508.

(21) This condition is only fulfilled by the electron-rich olefin/cyclobutane pairs. In the parent system the $CB^{\bullet+}$ + Et → $Et^{\bullet+}$ + CB is endothermic by more than 0.5 eV.

(22) For an excellent recent review see: Bauld, N. L. *Tetrahedron* **1989**, *45*, 5307.

(23) Almlöf, J.; Lund, A.; Thuomas, L.-A. *Chem. Phys. Lett.* **1975**, *32*, 190.

(24) (a) Bauld, N. L.; Pabon, R. *J. Am. Chem. Soc.* **1983**, *105*, 633. (b) Bauld, N. L.; Belville, D. J.; Chelsky, R.; Green, J. *J. Am. Chem. Soc.* **1983**, *105*, 2378. (c) Pabon, R. A.; Bauld, N. L. *J. Am. Chem. Soc.* **1984**, *106*, 1145. (d) Unfortunately, the authors did not report the activation energy for bond rotation in the π-complex (which would have proven that both bonds in $CB^{\bullet+}$ are indeed formed in concert), but the length of the short bonds in Bauld's complex (1.38 Å) indicate that this activation barrier would likely be higher than 7 kcal/mol.

(25) Chandra, A. K.; Bhanuprakash, K. *J. Mol. Struct. THEOCHEM* **1987**, *151*, 149.

(26) Lee, T.-S.; Lien, M. H.; Jen, S.-F.; Ou, M.-C.; Wu, H.-F.; Gau, Y.-F.; Chang, T.-Y. *J. Mol. Struct. THEOCHEM* **1988**, *170*, 121.

Table I. Total Energies in au of the Minima and Saddle Points Located on the UMP2/6-31G* Potential Energy Surface of $C_4H_8^{\bullet+}$

structure	UHF/6-31G*	UMP2/6-31G*	QCISD(T)/6-31G*	ZPE[a]
1. rhomboidal $cB^{\bullet+}$	−155.759 33	−156.269 15	−156.333 18	69.6
2. $(Et\cdots Et)^{\bullet+}$ (LC1)[b]	−155.772 32	−156.247 83	−156.323 74	67.8
3. transition state 1.–2. (TS1)[b]	−155.752 06	−156.241 59	−156.310 20	68.3
4. transition state 2.–5. (TS2)[b]	−155.759 20	−156.247 37	−156.314 50	67.4
5. 1-butene$^{\bullet+}$ ($1B^{\bullet+}$)	−155.809 43	−156.282 73	−156.353 54	68.7
6. *cis*-2-butene$^{\bullet+}$ ($2B^{\bullet+}$)	−155.824 55	−156.299 14	−156.370 01	
7. *trans*-2-butene$^{\bullet+}$ ($2B^{\bullet+}$)	−155.825 12	−156.299 47	−156.370 54	
8. isobutene$^{\bullet+}$ ($iB^{\bullet+}$)	−155.828 53	−156.302 01	−156.372 48	
9. ethylene + ethylene$^{\bullet+}$ [c]	−155.747 33	−156.214 77	−156.288 65	64.1

[a] Zero-point vibrational energy in kcal/mol calculated at the UMP2/6-31G* level. [b] See Figure 2. [c] Fragments at infinite distance. Energies corrected for the BSSE.

All the above calculations suffer from the drawback that the crucial points on their reaction pathways (minima and transition states) were not properly characterized by diagonalization of the force constant matrix. Also, they are limited to the single-determinant UHF level, which is known to overestimate the stability of structures with localized spin and charge such as the "long-bond" radical cations calculated to be the most stable geometries of various ionized alkanes.[27] For this reason and in an effort to extend our calculations on $CB^{\bullet+}$ described in the first part of this series,[28] we undertook a thorough reinvestigation of the Et + $Et^{\bullet+}$ cycloaddition and the rearrangement of the intermediate complex cation (or of $CB^{\bullet+}$) to the butene radical cations observed in many of the experiments described above.

In the following section we outline briefly the computational methods used in this work. In section 3 the results concerning the Et + $Et^{\bullet+}$ cycloaddition and in section 4 those for reaction leading to $1B^{\bullet+}$ are presented and discussed. In section 5 we propose a revised potential energy surface for the various $C_4H_8^{\bullet+}$ interonversions discussed above, and in section 6 we give a brief assessment of the minimal level of theory which we believe to be required for obtaining a qualitatively correct picture.

2. Computational Methods

The general computational strategy in exploring the P.E.S. of $CB^{\bullet+}$ has been outlined in part I of this study.[28] Unless stated otherwise, all calculations were performed with the 6-31G* basis set, which served for exploratory searches of the P.E.S. at the UHF level under various symmetry constraints, and/or allowing for full relaxation of the structures under study. Since the UHF level had not yielded an adequate description of the P.E.S. of $CB^{\bullet+}$,[28] all stationary points found in this way were reoptimized within UMP2 and characterized by performing a vibrational analysis at this level, which yielded also the values for the zero-point vibrational energy (if not stated explictly, all relative energies reported in this study are corrected to the ZPE). Finally, dynamic correlation effects were evaluated more definitely by single-point QCISD(T) energy evaluations at the UMP2 optimized structures. In the case of Et + $Et^{\bullet+}$ at infinite separation, the basis set superposition error (BSSE) was accounted for using the Boys–Bernardi counterpoise correction scheme.[29]

The UHF wave functions were found not to suffer from significant contamination by higher spin components in most of the species discussed below. Therefore the above methods (in particular the UMP2 calculations) are expected to yield reasonable results in such cases. One noteable exception to this rule was the ethylene dimer cation which consequently required special attention as described in the following section. Also our previous study[28] had indicated that adding more (polarization or diffuse) basis functions does not lead to significant changes of the relative energies both at the SCF and UMP2 levels. In the case of the transition state for the Et + $Et^{\bullet+}$ cycloaddition where an avoided surface crossing occurs, we also checked the adequacy of a single-reference approach by performing a CASSCF calculation (seven electrons in four bonding and four antibonding σ-MO's of the carbon frame). As suggested by a reviewer, we applied the same procedure to all important points of the presently investigated part to the $C_4H_8^{\bullet+}$ P.E.S. All calculations were done with the *Gaussian90* program package[30a] except for the CASSCF calculations, where GAMESS[30b] was used. The principal results obtained using the above described methods are summed up in Table I and compared to available experimental results in Table II.

Table II. Experimental and Calculated Relative Energies of Different $C_4H_8^{\bullet+}$ Species in kcal/mol[a]

reaction	exp	UHF[b]	UMP2[b]	UMP2[c]	QCISD(T)[c]
Et + $Et^{\bullet+}$ → $(Et\cdots Et)^{\bullet+}$ (LC1)	−18.3 ± 0.5[d,e] −15.8 ± 1.0[d,f]	−14.1	−16.6	−17.0	−18.2
Et + $Et^{\bullet+}$ → cyclobutane$^{\bullet+}$	≤−34[g]	−11.4	−20.8	−28.6	−22.4
$(Et\cdots Et)^{\bullet+}$ (LC1) → TS1		+12.0	+7.6	+4.3	+9.0
Et + $Et^{\bullet+}$ → 1–butene$^{\bullet+}$	−46[i]	−34.4	−41.5	−38.7	−36.8
$(Et\cdots Et)^{\bullet+}$ (LC1) → TS2		+8.9	−0.1	+0.7	+5.9
1-butene$^{\bullet+}$ → *trans*-2-butene$^{\bullet+}$ [h]	−14[i]	−9.8		−10.5	−10.7
trans → *cis*-2-butene$^{\bullet+}$ [h]	+1[i]	+0.4		+0.2	+0.3
trans-2-butene$^{\bullet+}$ → isobutene$^{\bullet+}$ [h]	+1[i]	+2.1		+1.6	+1.2

[a] All calculations were done with the 6-31G* basis set and are corrected for the zero point energy except where indicated. [b] At UHF optimized geometry. [c] At UMP2 geometry. [d] From supersonic beam experiments which are believed to yield ΔH(0K). [e] Reference 8a. [f] Reference 1. [g] Assuming I_a of cyclobutane ≤10.0 eV, see text. [h] Calculations not corrected for the ZPE. [i] From $\Delta H_f°$(298K).[35]

3. Et + $Et^{\bullet+}$ Cycloaddition Reaction

In previous calculations it was usually assumed that the $(Et\cdots Et)^{\bullet+}$ π-complex has rectangular[23,25] or trapezoidal[26] shape. However, for the case of $CB^{\bullet+}$, we had found that the trapezoidal minimum obtained at the SCF level disappears if correlation is included[28] and therefore we decided to impose no symmetry restrictions on the shape of the $(Et\cdots Et)^{\bullet+}$ complex. As a result, geometry optimizations starting from the different π-complex geometries described in the literature[23-26] led to a structure of C_2 symmetry, where the ends of the two ethylene moieties are linked by a long bond (1.917 Å by UMP2) and which is slightly puckered (cf. structure labeled LC1 in Figure 2). The P.E.S. was found to be very flat, and this led to displacements in successive optimization steps—even after the energy had converged to 10^{-7} hartree—which made it impossible to satisfy the corresponding convergence criteria. Therefore, the particularly "soft" puckering angle cannot be calculated very accurately.

Nevertheless, vibrational analyses at the UMP2 level revealed that LC1 is a true minimum with low-energy vibrations at 87, 117, and 186 cm^{-1}. Following these led to two saddle points, one

---

(27) Belville, D. J.; Bauld, N. L. *J. Am. Chem. Soc.* **1982**, *104*, 5700. See, however the recent work on propane radical cation by: Lunell, S.; Feller, D.; Davidson, E. R. *Theor. Chim. Acta* **1990**, *77*, 111.

(28) Jungwirth, P.; Čársky, P.; Bally, T. Preceding paper in this issue.

(29) Boys, S. F.; Bernardi, F. *Mol. Phys.* **1970**, *19*, 553.

(30) (a) Frisch, M. J.; Head-Gordon, M.; Trucks, G. W.; Foresman, J. B.; Schlegel, H. B.; Raghavachari, K.; Robb, M. A.; Binkley, J. S.; Gonzales, C.; DeFrees, D. J.; Fox, D. J.; Whiteside, R. A.; Seeger, R.; Melius, C. F.; Baker, J.; Martin, R. L.; Kahn, L. R.; Steward, J. J. P.; Topiol, S.; Pople, J. A. *Gaussian90*; Gaussian, Inc.: Pittsburgh, PA, 1990. (b) Schmidt, M. W.; Baldridge, K. K.; Boatz, J. A.; Jensen, J. H.; Koseki, S.; Gordon, M. S.; Nguyen, K. A.; Windus, T. L.; Elbert, S. T. GAMESS. *QCPE* **1990**, *10*, 52.

(31) Haselbach, E.; Schmelzer, A. *Helv. Chim. Acta* **1971**, *54*, 1299. Version for DOS-PC's (adapted to display split valence ab initio MO's by P. Jungwirth) is available from T. Bally upon request.

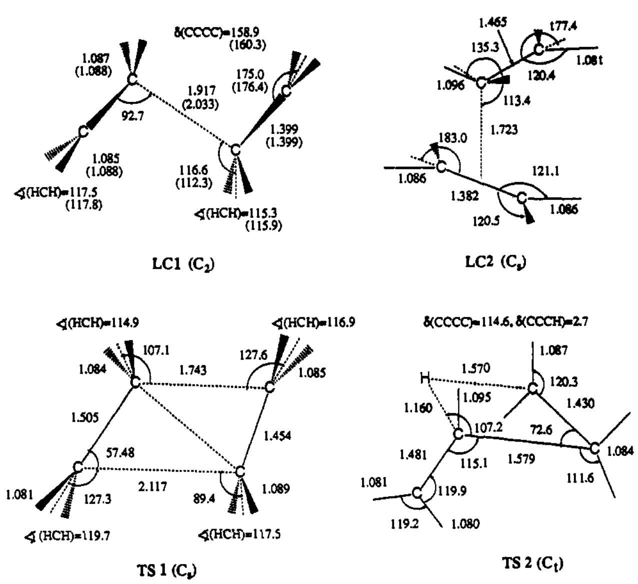

LC1 (C_2) LC2 (C_s) TS 1 (C_s) TS 2 (C_1)

Figure 2. UMP2/6-31G* geometries of the (Et···Et)$^{\bullet+}$ complexes LC1 and LC2, the transition state leading to cyclobutane radical cation (TS1), and the transition state for the 1,3 H-shift leading to 1B$^{\bullet+}$ (TS2). The numbers in parentheses for LC1 denote the QCISD/6-31G* equilibrium geometry (see text).

corresponding to LC1 with a planar carbon frame, 0.4 kcal/mol above LC1, the other to a D_{2h} rectangular π-complex with the two ethylene moieties separated by 2.66 Å, 1.4 kcal/mol above LC1 (4.7 kcal/mol at the QCISD(T) level), whose nature is that of a transition state for rotation around the long bond of LC1. At the UHF level this saddle point assumed a C_{2v} trapezoid geometry, 5.4 kcal/mol above LC1, whose geometry corresponds to that of the loose complex reported by Bauld et al.[24a]

A bothersome aspect of LC1 was the relatively large $\langle S^2\rangle$ value (0.91 instead of 0.75 for a pure doublet) of its UHF electronic wave function, which raised some doubts about the validity of using the MP2 method to recover dynamic correlation effects in this case. Indeed we found by coincidence that UMP2 optimization starting from a tetramethylene type geometry (cf. section 4) resulted in an entirely different (Et···Et)$^{\bullet+}$ equilibrium structure (LC2 in Figure 2) whose energy is 2.75 kcal/mol *lower* than that of LC1 but whose $\langle S^2\rangle$ value is 0.77. No similar minimum could be found on the UHF surface, but the UHF energy at the UMP2 geometry of LC2 is 3.03 kcal/mol *higher* than that of LC2.

Already at the MP4(SDQ) level, LC1 was again found to be more stable than LC2 by 0.14 kcal/mol, a difference which increased to 2.3 kcal/mol in favor of LC1 at the QCISD(T) level. We therefore think that LC2 represents an artifact which is due to the fact that the poor convergence of the MP series for the highly contaminated UHF wave function of LC1 puts this species at a spurious disadvantage of ≈5 kcal/mol relative to LC2 at the UMP2 level. To our knowledge this is the first example of a polyatomic molecule where this effect leads to such a profound change in the shape of a P.E.S. However, the fact that LC1 is the energetically favored (Et···Et)$^{\bullet+}$ structure at the QCISD(T) level, where high-spin contaminations are largely eliminated from the electronic wavefunction, indicates that LC1 rather than LC2 is the reference structure of choice. Furthermore, complete reoptimization of LC1 at the QCISD level (where analytical derivatives are available in *Gaussian*) led only to minor changes in the geometry (cf. numbers in parentheses in Figure 2) and to a drop of the QCISD(T) energy by only 0.46 kcal/mol relative to that at the UMP2 geometry. This shows that the latter can be regarded as realistic in spite of the pronounced high-spin contamination of the underlying UHF wave function.

The dissociation energy D_e of the (Et···Et)$^{\bullet+}$ complex calculated on the basis of the LC1 structure is 18.2 kcal/mol at the QCISD(T) level. The latter number is in excellent agreement with that obtained by Ceyer et al. (18.2 ± 0.5 kcal/mol)[8a] but higher than that obtained in the more recent study of Ono et al. (15.8 ± 1 kcal/mol),[1a] where contributions due to trimer complexes were carefully excluded. Since even the QCISD(T) calculations do not account for 100% of the attractive dispersion forces (dynamical correlation) to the binding energy of the (Et···Et)$^{\bullet+}$ complex, it appears that this quantity must be slightly overestimated already at the SCF level. Again, CASSCF calculations showed that nondynamic correlation effects cannot be responsible for this, since a single determinant accounts for more than 92% of the MCSCF expansion while the second most important configuration contributes less than 4%.

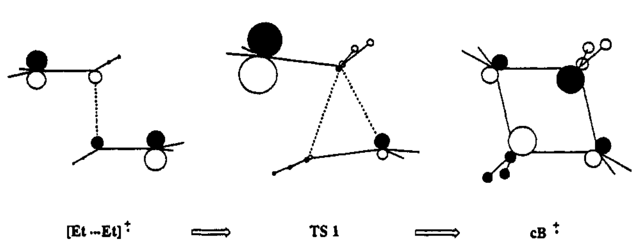

Figure 3. MOPLOT[31] illustration of the changes in the geometry and in shape of the HOMO during the Et + Et$^{\bullet+}$ cycloaddition.

The (Et···Et)$^{\bullet+}$ → CB$^{\bullet+}$ ring closure, which is nearly thermoneutral at the UHF level, becomes exothermic by 11.2 kcal/mol in UMP2, which can, however, be attributed in part to the spurious destabilization of LC1 at this level (see above). QCISD(T) calculations predict ΔH for this process to be −4.2 kcal/mol, which means that it is feasible in principle. Due to the strongly nonvertical nature of the CB ionization process, $\Delta H_f°$ of CB$^{\bullet+}$ cannot be determined accurately, and it is therefore difficult to relate the above numbers to experiment. If we assume that I_a(CB) ≤ 10 eV,[11] this leads to an experimental estimate for the enthalpy change for the overall Et + Et$^{\bullet+}$ → CB$^{\bullet+}$ reaction of ≤−34 kcal/mol, compared to which the calculated values (cf. Table II) are significantly too low. Due to the large discrepancies between the UHF- and UMP2-optimized geometries of CB$^{\bullet+}$,[28] it is difficult to pinpoint the error in this case.

The search for the transition state linking the (Et···Et)$^{\bullet+}$ complex to CB$^{\bullet+}$ turned out to be rather tedious but resulted eventually in the structure labeled "TS1" in Figure 2, whose energy at the QCISD(T) level is 9.0 kcal/mol higher than that of the π-complex LC1. The vibrational analysis revealed a single mode with a negative frequency of −450 cm^{-1} leading to rhomboidal CB$^{\bullet+}$. Figure 3 illustrates the change in shape of the singly occupied HOMO in the course of the (Et···Et)$^{\bullet+}$ → CB$^{\bullet+}$ interconversion. It shows the nearly complete localization of spin and charge at the transition state which is necessary to avoid the state crossing due to the net change of phase along the ethylenic C–C bonds in the course of the reaction. In view of this avoided crossing, we performed supplementary CASSCF calculations as described in section 2, but those indicated that the ground-state wave function at the transition state is 93% single determinantal[32] while the second most important configuration contributes less than 2%.

4. Rearrangement to 1-Butene Radical Cation

In spite of the low activation barrier for formation of CB$^{\bullet+}$ from (Et···Et)$^{\bullet+}$, this reaction is not observed in the gas phase[2] or in condensed-phase experiments[16] involving ionized Et$^{\bullet+}$. Instead, different butene radical cation isomers are formed spontaneously, which suggests that another transition state of lower energy exists which leads to this part of the $C_4H_8^{\bullet+}$ P.E.S. We assumed that a 1,3 hydrogen shift leading to the radical cation of 1-butene (1B$^{\bullet+}$) would be the most favorable reaction

---

[32] CIS/6-31G* calculations showed that the first excited configuration lies >3 eV above the ground state at this geometry.

Table III. Relative Energies in kcal/mol and Character of Different Tetramethylene Radical Cations in C_{2v}, C_{2h}, or C_s Symmetry, Respectively

SOMO	sym	UHF[a]	UMP2[b]	(identity);[c] character	SOMO	sym	UHF[a]	UMP2[b]	(identity);[c] character
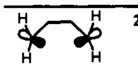	$^2A_1$	+0.9	−28.6	(UHF, trapezium; UMP2, rhombus); collapses to $cB^{\bullet+}$ minimum	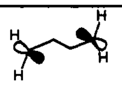	^2A_g	+47.7	+80.1	(NI = 2); excited state of LC1
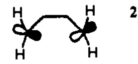	$^2B_2$	+5.4[d]	+1.4[e]	(NI = 1); TS for rotation around the long C–C bond of LC1		^2B_u	+0.1	+0.4	(UHF, NI = 0; UMP2, NI = 1); TS for interconversion of two puckered forms of LC1
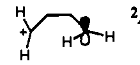	$^2A''$	+14.2	+8.6	(NI = 2); collapses to LC2 upon loss of symmetry[f]	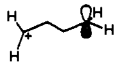	$^2A''$	+11.4	+7.2	(NI = 2); collapses to LC1 upon loss of symmetry[f]
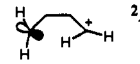	$^2A'$	+15.0	+17.8	(NI = 2); collapses to LC2 upon loss of symmetry[f]	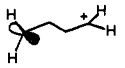	$^2A'$	+13.2	+17.2	(NI = 1); TS for rotation around one of the short C–C bonds of LC1
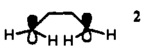	$^2B_1$	+30.3	+15.7	(NI = 1); TS for conrotatory twisting of both CH_2 groups in $cB^{\bullet+}$	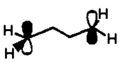	^2B_g	+30.6	+15.6	(NI = 1); TS for concerted twisting of both CH_2 groups in LC1
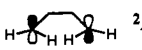	$^2A_2$	+49.0	+32.8	(NI = 2); excited state of $^2B_1$	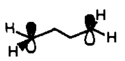	^2A_u	+40.1	+22.9	(NI = 1); excited state of ^2A_u

[a] UHF/6-31G*//UHF/6-31G* energy relative to $(Et\cdots Et)^{\bullet+}$. [b] UMP2/6-31G*//UMP2/6-31G* energy relative to $(Et\cdots Et)^{\bullet+}$. [c] NI = number of imaginary frequencies (at both levels if not specified otherwise). [d] Corresponds to Bauld's loose complex.[24a] [e] Attains D_{2h} symmetry upon UMP2 optimization. [f] See text.

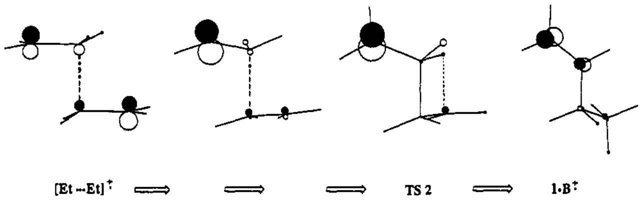

Figure 4. MOPLOT[31] illustration of the changes in the geometry and in shape of the HOMO during the 1,3 H-shift leading from $(Et\cdots Et)^{\bullet+}$ to $1B^{\bullet+}$.

path starting from the $(Et\cdots Et)^{\bullet+}$ complex, and we discovered indeed that shortening the long bond while optimizing all other variables leads smoothly to a low-lying saddle point (labeled "TS2" in Figure 2) which at the UMP2/6-31G* level has one negative frequency of −396 cm^{-1} corresponding to the reaction vector for the 1,3 hydrogen shift.[33] By following the reaction backward from this transition state to the $(Et\cdots Et)^{\bullet+}$ complex, staying always on the bottom of the P.E.S. valley linking the two structures, we found that the critical geometry change is a twisting of one of the ethylene's C–C bonds which results in a localization of spin and charge (cf. Figure 4). The CH_2 group which eventually "picks up" the migrating hydrogen atom has essentially turned into a carbonium ion center by the time the system has reached the transition state.

The calculated activation energy for the $(Et\cdots Et)^{\bullet+} \rightarrow 1B^{\bullet+}$ rearrangement (5.9 kcal/mol at the QCISD(T) level) is significantly lower than that leading to $CB^{\bullet+}$, in accord with experimental observations. However, our calculations do not support the conclusion of van der Meij et al., who claimed that the barrier separating the $(Et\cdots Et)^{\bullet+}$ collision complex from the tightly bound butene cations exceeds the separated fragments Et + $Et^{\bullet+}$ in energy.[8b] Even if we take the latest experimental value of 15.8 kcal/mol for the dissociation energy of $(Et\cdots Et)^{\bullet+}$ as a reference,[1a] TS2 still lies some 10 kcal/mol lower, too much to explain in terms of an error at this level of theory.

Since it has been observed that not only the $(Et\cdots Et)^{\bullet+}$ complex but also $CB^{\bullet+}$ yields $1B^{\bullet+}$ (and subsequently other butene radical cations) upon ionization close to threshold,[3-7] we searched also for a pathway linking $CB^{\bullet+}$ to $1B^{\bullet+}$. In view of the numerous suggestions[1c,7,8] postulating that this reaction proceeds via an intermediate tetramethylene radical cation ($tM^{\bullet+}$), we initially focused our attention to this type of molecule. We started out by a set of optimizations under various assumptions with regard to the symmetry (C_{2v} or C_s) and electronic structure of different conceivable $tM^{\bullet+}$ species, as shown in Table III. The most stable one of these (^2B_u) is the transition state for planarization of puckered LC1, but the central C–C bond of this species is so long that it is better regarded as a loose π-complex than a (tightly bound) $tM^{\bullet+}$.

The cis-form of $^2A''$ is the species which collapsed (and hence led us) to the UMP2 global minimum for $(Et\cdots Et)^{\bullet+}$, i.e. LC2, upon unconstrained optimization (cf. previous section). The same happens to $^2A'$, which mixes with the more stable $^2A''$ upon loss of symmetry. In contrast, the trans-forms of $^2A'$ represent the transition state for rotation around one of the short C–C bonds of LC1 while $^2A''$ collapses to the latter upon loss of symmetry. Finally, the planar $^2B_1$ (cis) and ^2B_g (trans) states were found to be saddle points for synchronous rotation of two C–C bonds in $CB^{\bullet+}$ or LC1, respectively, while the corresponding A-states were much higher in energy.

Thus we are forced to conclude that—contrary to widespread belief[1c,7-9]—*no tightly bound tetramethylene cation is involved in the rearrangement of $(Et\cdots Et)^{\bullet+}$ or ionized cyclobutane to the radical cation of 1-butene*. Apparently $tM^{\bullet+}$ is even more elusive than the corresponding neutral biradical, which is barely stable to dissociation or cyclization.[34]

In order to complete the picture, we also calculated the radical cations of the three butenes at the same level of theory. The UMP2 geometries are shown in Figure 5 while the corresponding energies are listed in Table I. In Table II we compare some of the calculated relative energies of the species involved in this study to experimental values. It can be seen that agreement between theory and experiment is satisfactory, although not always optimal at the highest level of computation applied in this work.

5. Revised Potential Energy Surfaces

In Figure 6 we present a revised version of Figure 1 which takes into account the results of the present study. Again, we have used experimental thermochemical data for Et + $Et^{\bullet+}$ and the butene radical cation to "anchor" the P.E.S. on a $\Delta H_f°$ scale. In the case of $CB^{\bullet+}$, the dotted line corresponds to the species

---

(33) In view of recent findings (Glukhovtsev, M.: Private communication) indicating that at least two sets of p-functions on hydrogen are needed to correctly model situations where multiply coordinated hydrogens are involved, we reoptimized the saddle point TS2 at the UHF level with a 6-31G* basis set augmented by two sets of p-functions with exponents 2.20 and 0.55 on the bridging hydrogen atom. Starting from UHF/6-31G* geometry, the energy of TS2 decreased by only 0.4 kcal/mol and the geometry underwent no significant changes (0.06 Å for the long bonds to the bridging hydrogen, all other bondlengths <0.04 Å).

(34) Bernardi, F.; Bottoni, A.; Celani, P.; Olivucci, M.; Robb, M. A.; Venturini, A. *Chem. Phys. Lett.* **1992**, *192*, 229.

(35) Lias, S. G.; Bartmess, J. E.; Liebman, J. E.; Holmes, J. L.; Levin, R. D.; Mallard, W. G. *J. Phys. Chem. Ref. Data* **1988**, *17*, Supplement No. 1.

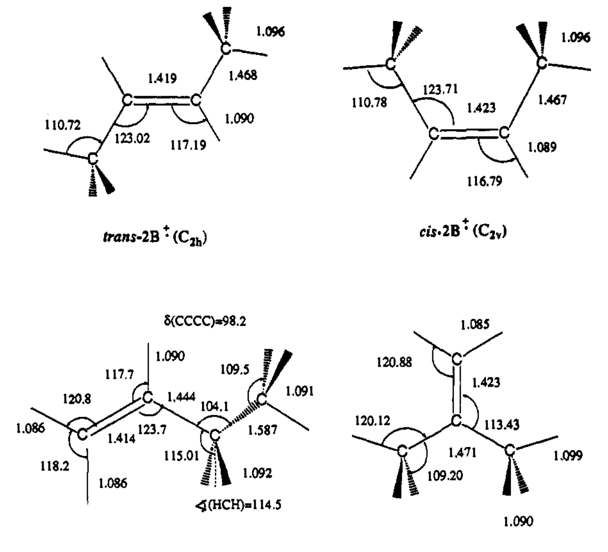

trans-2B$^{+\cdot}$ (C_{2h}) *cis*-2B$^{+\cdot}$ (C_{2v})

1-B$^{+\cdot}$ (C_1) iB$^{+\cdot}$ (C_{2v})

Figure 5. UMP2/6-31G* equilibrium geometries of four different butene radical cations.

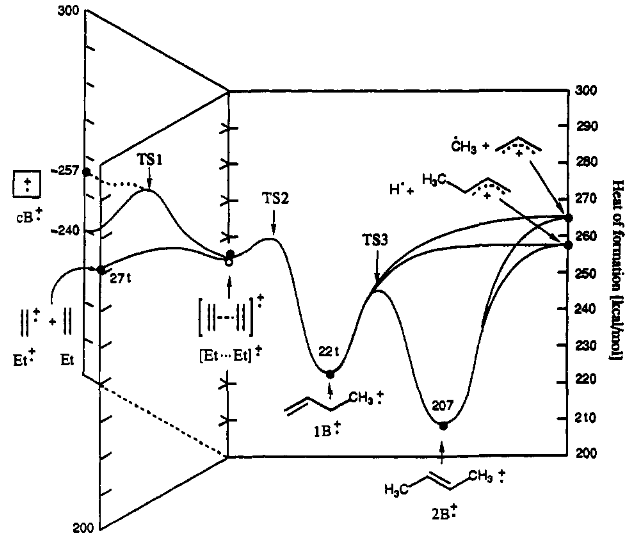

Figure 6. Revised picture of the $C_4H_8^{\cdot+}$ potential energy surface. Filled dots correspond to experimental thermochemical data.[1a] For discussion see text.

obtained by threshold photoionization of CB[2b,c] while the solid line is for the relaxed ground state of the radical cation according to our previous calculations.[28] With regard to the transition state for the $1B^{\cdot+} \rightarrow 2B^{\cdot+}$ conversion (TS3), we based our estimate on the recent work of Clark,[36] who had found a value of 29.6 kcal/mol for the automerization of propene radical cation. Due to the ≈15 kcal/mol exothermicity of the 1,3 H-shift in the case of $1B^{\cdot+}$, it was assumed (following the Bell–Evans–Polanyi principle) that this barrier is lowered to about 25 kcal/mol.

On the basis of this picture, many of the experimental observations outlined in the Introduction can be explained while some new questions are raised. First we note that the often invoked $tM^{\cdot+}$ is most probably not an intermediate in any of the $C_4H_8^{\cdot+}$ interconversions discussed in this study. Figure 6 suggests that the $CB^{\cdot+} \rightarrow 1B^{\cdot+}$ reaction proceeds actually in two steps, the first one being a "partial cycloreversion" to $(Et\cdots Et)^{\cdot+}$ which is followed by a 1,3 H-shift, thereby bypassing the higher energy $tM^{\cdot+}$. Secondly, TS3 for the $C_4H_6^{\cdot+}$ interconversion lies well below TS1 and TS2, which explains why no $1B^{\cdot+}$ was found upon neutralization of CB or Et ionized in high-pressure gas-phase experiments.[37] Apparently the transition state for CH_3 migration to form $iB^{\cdot+}$ lies also below TS2, and therefore the 80:20 ratio of 2B to iB detected after neutralization reflects the equilibrium concentrations of the corresponding radical cations, which are of very similar stability.[1a]

Thirdly, the behavior of $CB^{\cdot+}$ in condensed-phase experiments can also be rationalized on the basis of Figure 6. Clearly, relaxed $CB^{\cdot+}$ lies in a well which it cannot escape at the low temperature prevailing in the Freon matrix experiments[16] while upon photoexcitation[17] the barrier separating it from the other $C_4H_8^{\cdot+}$ isomers can be crossed. Whether the photorearrangement proceeds also via $(Et\cdots Et)^{\cdot+}$, which cannot relieve itself of the excess energy rapidly enough to escape projection across TS2 or whether in this case a $tM^{\cdot+}$ species is actually involved at some stage cannot be decided on the basis of the present results. In any event, the low calculated barrier associated with TS2 explains why the ion–molecule reaction between Et and $Et^{\cdot+}$ proceeds spontaneously in Freon matrices.[15]

On the other hand, the excess energy imparted onto the incipient $CB^{\cdot+}$ upon threshold photoionization[6] in the gas phase suffices apparently to project it over TS1 into the region where it rearranges spontaneously to the butenes prior to thermalization. This latter feature is not borne out quantitatively by Figure 6, which is due to the fact that the position of TS1 on a $\Delta H_f°$ scale depends critically on the exact position of $(Et\cdots Et)^{\cdot+}$ relative to the separated fragments. In any event, TS1 is certainly not much lower in energy than CB photoionized at 1165 Å, and our data suggest that, if $CB^{\cdot+}$ could be formed with even less excess energy, it might actually withstand rearrangement even in the gas phase.

In sum, our calculations indicate that the $(Et\cdots Et)^{\cdot+}$ π-complex plays a pivotal role in the various $C_4H_8^{\cdot+}$ rearrangements observed in different experiments. Conversely, the ubiquitous $tM^{\cdot+}$, whose existence formed the basis for several model calculations,[7,9] does not appear to be involved in any thermal process on this surface. A very low barrier separates $(Et\cdots Et)^{\cdot+}$ from $1B^{\cdot+}$ while slightly more energy is needed to cross over to $CB^{\cdot+}$, which explains the absence of this species in the gas-phase reneutralization experiments.

6. Reliability of Theoretical Models

Since the level of theory used in this study (QCISD(T)/6-31G*//UMP2/6-31G*) can presently not be applied to systems much larger than C_4H_8, it is of interest to know whether less expensive calculations are also capable of yielding qualitatively correct results. Inspection of Table II shows that geometry optimizations at the SCF level followed by single-point calculations at a correlated level of theory may yield adequate results provided the relative energies of different stationary points are not grossly changed upon account for correlation. If such behavior is observed (as in the case of $CB^{\cdot+}$ [28]), reoptimization at a correlated level is indicated if a realistic picture of the P.E.S. is desired.

A particular problem surfaced during the search for the $(Et\cdots Et)^{\cdot+}$ equilibrium structure where entirely different minima were found at the UHF (LC1) and UMP2 levels (LC2). We attributed this to the poor convergence of the MP series for high-spin contaminated UHF wave functions (such as LC1), which makes the UMP2 model favor species (like LC2) which correspond to nearly pure spin states in a UHF description. This is in contrast to results obtained at the UHF level, where high-spin contamination may actually lead to an artificial energy lowering. Consequently, great caution is indicated in UHF and UMP2

---

(36) Clark, T. *J. Am. Chem. Soc.* **1987**, *109*, 6838.

(37) See footnote 13 in ref 6.

calculations involving alternative structures with very different $\langle S^2 \rangle$ expectation values.[38]

The example of $(Et\cdots Et)^{\bullet+}$ also showed that it is very difficult to make accurate predictions of the equilibrium geometries of loose complexes but that this is not important if only the energies relative to more tightly bound isomers are of interest. It may be advisable to freeze some of the very soft modes of such species after rough convergence and treat those separately after complete optimization of all other degrees of freedom.

7. Conclusions

We have shown in the present study that an ethylene dimer cation $(Et\cdots Et)^{\bullet+}$ is the primary product of the ion–molecule reaction between ethylene and its radical cation. The same species is also involved in the rearrangement of ionized cyclobutane to butene radical cations, which does not appear to proceed via a tetramethylene cation, as postulated repeatedly. The calculated $C_4H_8^{\bullet+}$ potential energy surfaces are in good accord with most experimental observations although some small quantitative discrepancies remain which may be accounted to deficiencies inherent even in the highest level of theory which we could apply systematically to the species studied in the present work.

Acknowledgment. This work is part of Project No. 20-34071.92 of the Swiss National Science Foundation, who also made it possible for P.J. to spend six months in Fribourg for the purpose of the collaboration whose results are reported in this study. We are very indebted to IBM Switzerland for the loan of an RS/6000 workstation, without which this project would have been impossible to carry out. We would like to thank Prof. Edwin Haselbach (University of Fribourg) for his encouragement and Prof. Petr Čársky (Academy of Sciences of the Czech Republic) for valuable comments.

---

(38) Perhaps the newly emerging generation of ab initio programs which allow for ROHF/MBPT calculations[39] will lead out of this impasse which can presently only be escaped by taking recourse to a level of theory (such as the QCISD(T) coupled cluster approach used in the present paper) where it does not longer matter very much whether the zero-order SCF wave function is of restricted or unrestricted nature but which generally does not allow for geometry optimization, let alone vibrational analysis of stationary points.

(39) CADPAC 5.0 (Amos, R.: Personal communication); ACES II (Stanton, J. F.; Gauss, J.; Watts, J. D.; Lauderdale, W.; Bartlett, R. *Int. J. Quantum Chem. Symp.* **1992**, *26*, 894).